Artificial Neural Network based fault diagnosis in an isolated photovoltaic generator.

Ousmane W. COMPAORE[1,2], Galeb HOBLOS[1], Zacharie KOALAGA[2]
cwousmane@yahoo.fr , o.compaore@esigelec.fr

Normandy University, UNIROUEN, ESIGELEC, Institut de Recherche en Systèmes Electroniques Embarqués, 76801 Ave Gallilé. Rouen France[1]; University Joseph Ki-ZERBO. Faculty of Science and Technology. Laboratoire de Matériaux Environnement. 03 BP 7021, Ouagadougou 03. Burkina Faso[2]

Abstract. The efficiency of a photovoltaic (PV) system depends not only on environmental and operating conditions, but also on manufacturing. This dependence is intrinsically linked to parameters such as R_s, R_{sh}, N_{cell} or I_{ph}. In other words, a good PV generator (PVG) is one where the power delivered by the PVG is maximum whatever the conditions of use. In this article, we expose a model of PVG, as well as some faults that affect its optimal functioning. Given the complexity and the multitude of diagnosis methods, we have opted for the artificial neural networks (ANN) approach to detect, identify and locate certain faults that hinder its good performance. Once the correct diagnosis is made, it will be up to the maintenance technicians to take the necessary actions.

Keywords: Photovoltaic Generator, PVG, fault, classification, detection, diagnosis, Artificial Neuron Networks (ANN), Remaining useful life (RUL).

1 Introduction

The photovoltaic generator (PVG) is a renewable, inexhaustible and non-polluting source of energy. The increase in energy demand means that the use of renewable energies is increasing significantly around the world. This strong growth in demand for electrical energy, mainly in remote, desert and even mountainous regions, creates problems for both the design, construction and maintenance of PVG [1].

The robust, reliable, high performance PVG must be able to cope with faults [2] through proactive and tailored maintenance.

A.E. T. Maamar and al (2018) in [11], were specifically interested in detecting and classifying faults of a PVG using the neural approach. The performance of the neural approach was analysed on the basis of a comparison with the threshold method. Both methods are based on generating input residuals between healthy and failing modes. It was then necessary to set a threshold for each fault with the threshold method, which was not the case for the method based on the artificial neural network learning algorithm. But in [12], we note that a PVG could be subjected during its operation to various faults requiring a certain approach to detect them. Also they were interested specifically in the detection and location of faults of the PVG by the neural approach. Hadjib and al., in [13], analyzed the conditions of a good PV installation, so that the power delivered by the PVG would be maximum, whatever the conditions of use. Also, they

JRI 2021, November 11-13, Bobo-Dioulasso, Burkina Faso

DOI 10.4108/eai.11-11-2021.2317977

used artificial neural networks (ANN) as an approach to track the maximum point of power regardless of where they were used and operating conditions

There are many works which propose different methods to diagnosis PVG faults [4], [8], [9], but they are not all suitable to diagnosis all faults simultaneously. The obligation for [11] to set a detection threshold according to the nature of the fault, leads us to other diagnosis methods based on the ANN.

This article presents a model as close as possible to the real behavior of a PVG based on a Bishop model [7] from its basic cell to the PVG. We will base our approach, on the knowledge of the faulty behavior of the cell up to the PVG, to establish a global fault scenario [6], in order to establish a relation between the fault and the symptoms presented in characteristic IV of the PVG and which seriously affects production performance [14].

The implementation in MATLAB / Simulink will simulate the healthy and degraded behavior of PVG. We will apply a diagnosis method whose principle is based on artificial neural networks, for the detection, identification and localization of defects.

In section 1, we will introduce the problems related to fault diagnosis in PVG, before stating the problem statement in section 2. The PVG application model will be presented in section 3. We will present some faults of PVG in section 4, before presenting the approach by ANN in section 5. The interpretation of the simulation results is summarized in section 6. Finally, in section 7, we will conclude on the proposed diagnosis method and suggest some perspectives.

2 Problem statement

The first objective of this work is to present a model as close to the reality of a PVG, as well as some inherent faults in the proper functioning of all complex industrial processes. The second objective of the work is to implement a diagnosis method based on artificial neural networks, able of identifying said faults in the PVG. The application of the fault detection and isolation (FDI) method on this industrial system which exhibits peculiarities of non-linearities and faults that can significantly affect its operating performance. The simulation results on the detection of faults in accordance with the incidence matrix will make it possible to isolate any faults. Ultimately, this will make it possible to undertake corrective or predictive maintenance actions resulting from the diagnosis made.

3 PVG model

When the PV cell is occulted, it operates in the reverse regime of zone C [5]. Standard cell models, one diode or two diodes [3], represent only normal cell models, i.e., in zone A of the operating characteristic of Figure 1. This does not take into account the avalanche effect of the cell. This function, which can only be explained in the failed mode of the cell or field, requires a model that can describe the entire cell characteristic in the three [4] areas of Figure 1.

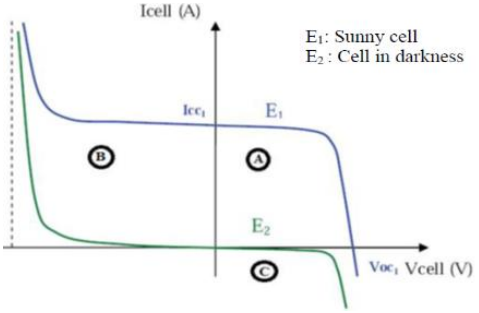

Fig.1. Complete characteristic I-V of PV cell

In normal operation, the cell operates in zone A where the operating point is within the limit defined by its I_{cc1} short circuit current based on its V_{oc1} circuit voltage. However, in abnormal operation, the cell may be forced in the negative region of its voltage (zone B) and the negative current region (zone C). The cell will be damaged when the rupture voltage is reached.

The avalanche effect of the cell is considered only in the Bishop model [7] presented in Figure 1. It is improved by the addition of the nonlinear multiplier factor *M(V1)* representing the mass avalanche effect with shunt resistance [4, 7, 8, 9]. Its electrical pattern is given by figure 2, and the mathematical model is given by relation (1):

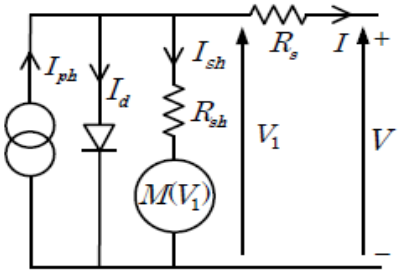

Fig.2. Bishop model of PV cell

$$I = I_{pv} - I_0\left[\exp\left(\frac{V+R_sI}{V_t}\right) - 1\right] - \frac{V+R_sI}{R_p}\left[1 + k\left(1 - \frac{V+R_sI}{V_b}\right)^{-n}\right] \quad (1)$$

where

$$I = I_{pv} - I_0\left[\exp\left(\frac{V+R_sI}{V_t}\right) - 1\right] - \frac{V+R_sI}{R_p}M(V_1) \quad (2)$$

$$\text{With } M(V_1) = 1 + k\left(1 - \frac{V+R_sI}{V_b}\right)^{-n} \quad (3)$$

k : Bishop's adjustment coefficient ($3{,}4 \leq k \leq 4$)
n : Bishop's adjustment coefficient ($n \cong 0{,}1$)
V_b: cell clacking voltage ($-30 \leq V_b \leq -10$)

This model called Bishop with its eight parameters $a, I_d, R_s, R_{sh}, k, n, V_b$ *et* I_{ph} takes into account the avalanche effect of the diode, which passes successively from operating areas A, B

to C in figure 2. It is a model of PV cell study, very close to reality, which is sometimes in generator, if it is well sunny and sometimes in receptor, when it is under shade.

The parameter a or ideality factor of the diode, depends intrinsically on the nature of the used semiconductor [3].

From the model of the cell presented above to the PV field through the module, the whole is subject to the same conditions of temperature and sunshine [5]. The equivalent circuit of the PVG, with an N_s number of serial-mounted modules and an N_p number of parallel-mounted modules showns in Figure 3, with the relationships (4) to (7) to establish the current and voltage of the PVG created [4, 10, 11]. We get for healthy mode:

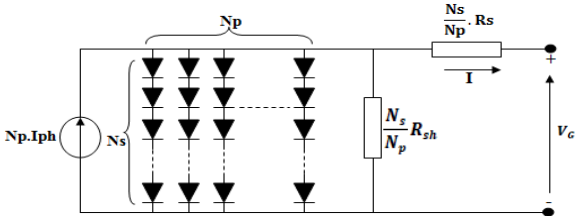

Fig.3. PV generator model.

Thus, we obtain successively:

- from cell to module through relations (4);

$$\begin{cases} I_c = I \\ V_m = N_{cell} * V \end{cases} \quad (4)$$

- from module to string by relations (5);

$$\begin{cases} I_{stg} = I \\ V_{stg} = N_s * V_m \end{cases} \quad (5)$$

- from string to field by relations (6);

$$\begin{cases} I_G = N_p * I_{stg} \\ V_G = V_{stg} \end{cases} \quad (6)$$

- finaly from the field to the generator by the relations (7).

$$\begin{cases} I_G = N_p * I \\ V_G = N_s * N_{cell} * V \end{cases} \quad (7)$$

with the following notations:

- K_i: the current / temperature coefficient of short-circuit;
- K_V : the open circuit voltage/temperature coefficient;
- $T\ and\ T_n$ are the current and nominal temperatures
- $G\ and\ G_n$ are the current and nominal illuminance;
- I_{phn} : the nominal current of the PV cell, given under nominal conditions $T = 25℃\ and\ G = 1000\mathrm{W/m^2}$;
- I_c : current supplied by PV cell;

- I_{stg} : PV module current;
- I_G : generator current or PV field;
- I_d: the current in the diode;
- I_0: the saturation current of the diode;
- I_{scn} : the rated short-circuit current at standard test conditions (STC) $T = 25℃\ and\ G = 1000\mathrm{W/m^2}$;
- V_t: the thermal tension of the panel;
- V_{ocn} : the nominal open circuit voltage;
- V voltage at the terminals of PV cell;
- V_m: voltage at the terminals of PV module;
- V_{stg}: voltage at the terminals of string;
- V_G: voltage at the terminals of generator or PV field;
- k_b : Boltzmann's constant;
- q : the charge of the election;
- N_{cell} : number of cells in series in a module;
- N_s: number of serial modules in a string;
- N_p: number of strings in parallel in the PV generator;
- R_s: series resistance of the cell which depends on the materials used to construct the cell and whose effect is greatest in the voltage source operating region;
- R_{sh} : parallel resistance whose effect is greatest in the current source operating region;
- a: coefficient of ideality of diode;
- k : Bishop's adjustment coefficient;
- n : Bishop's adjustment coefficient;
- V_b: the breakdown voltage of the cell.

The characteristic I-V in healthy operation mode can be done on the basis of a single PV cell. This is achieved by the relation (7). Here, the behaviour of all the cells is identical, which causes the blocking of the bypass diode and the conduction of the anti-return diode.

The simulation of healthy mode is done with modules of 36-cell. The generators below, are configured by $N_s * N_p$ modules, one module, two modules, four modules, eight modules and finally 16 modules.

Below, the simulation of healthy mode with modules of 36-cell in Figure 4, was done for: $R_s = 0.015\ \Omega;\ R_{sh} = 700\ k\Omega;\ T = 25°C\ et\ G = 1000W/m^2$:

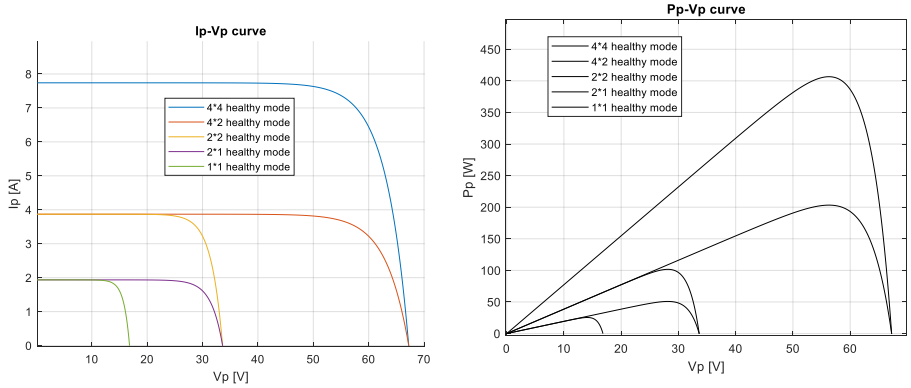

Fig.4. Healthy mode: characteric of Current and Power

4 The PVG faults

The failure mode is a particular case of the one proposed to model a healthy PV field. Also, we simulated it under Simulink, in order to have access to all components of the system. This allows to introduce the type of considered faults $R_s, R_{sh},\ N_{cell},\ I_{ph}, T\ or\ G$.

4.1 Considered faults

Simulation of the behaviour of a PV field for a comprehensive fault scenario shows that it is possible to identify potential symptoms that can be used to overcome the nature of faults. Also, the combination of the symptoms identified, also known as faults signature, allows the identification of the fault or a group of faults responsible for the behaviour examined [4]. On the characteristic of Figure 5, the following five zones can then be identified.

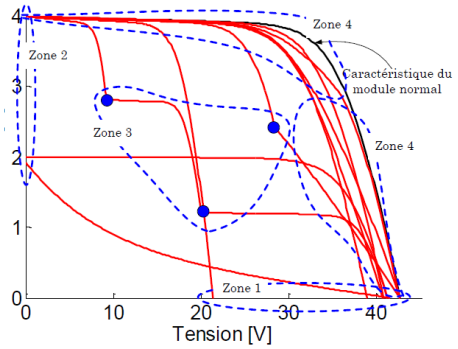

Fig. 5. I-V characteristic in healthy mode (black) and failure mode (red)

- The first obvious fault, which once appeared may suggest the presence of a failure, is the loss of power produced. Because this is not always true, however, certain faults do not lead to any loss of power. This is the case when the bypass diode is disconnected.
- The second fault in "zone 1" is the known difference between the open circuit voltage of the PV system in normal operation and the failed circuit voltage in zone 1 of figure 5. Like a module ripped off (R_s, R_{sh}) or bypassed, or a temperature rise (T).
- The third fault in "zone 2" is the known difference between the short circuit current of the PV system in normal operation and the failed current in zone 2 of figure 5. Like the loss of a module of string (R_s, R_{sh}) or a bad sunshine (G).
- The fourth fault in "zone 3" refers to the abrupt deviation of the characteristic I-V which leads in the latter to one or more inflection points in zone 3 of figure 5. Like losing a set of modules in a string (N_{cell}, R_s, R_{sh}).
- The fifth fault in "zone 4" refers to the deviation of the slope of the failing I-V characteristic from that in healthy operation. There is no deviation if the voltage and current drop profile is constant throughout the I-V curve. Otherwise, attention will be given:
  - ✓ to the voltage drop profile in vertical zone 4 of figure 5, corresponding to an increase in the serial resistance (R_s);
  - ✓ to the profile of the current fall in zone 4 horizontal of figure 5, corresponding to a decrease in shunt resistance (R_{sh}).

4.2 Signature table

The results of simulations of [3] to [5] allow us to establish the simplified table of faults given in table 1. The code generated will be used for interpretation during simulation.

Table 1: Signature of faults

Code	P	V	I	Default Designation
000	0	0	0	Healthy mode
001	0	0	1	Mismatch type shade or sunshine
010	0	1	0	Short-circuited or reverse module
011	0	1	1	Mismatch type partial shade, or dirt
100	1	0	0	Bypass or Mismatch type Rp or Rs
101	1	0	1	Bypass or Mismatch type Rp or Rs
110	1	1	0	Mismatch type Rs
111	1	1	1	Fault nature is Unknown

4.3 Generating matrix input

Simulink simulation was used to replicate the behaviour of our PVG, to extract the input matrix [P, V, and I] as matrix [201*3]. For each of the faults introduced, we could feed each simulation base. In the synoptic of the Figure 6 below, we summarize the construction of the database used to feed the inputs of the ANN algorithm.

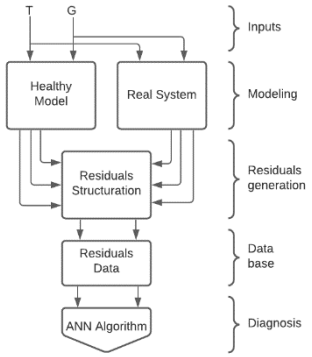

Fig. 6. Synoptic of construction of database used.

5 Proposed approach

Nowadays, the artificial neural network is an essential tool used in many research activities for complex industrial systems. One of the advantages of using neural networks to detect failures in complex systems is that they can interpret measurement data. Because a neural network, is able to generalize a obtained model. Error tolerance, which characterizes the neural network, effectively treats model errors. In addition, he can perform non-linear mapping and learn dynamic behaviours in order to generalize the obtained models.

For data processing, the use of ANN is an interesting approximation approach for systems that are difficult to model using conventional statistical methods [3].

5.1 The architecture of a neuron

Figure 7 shows an artificial neuron receiving signals from the environment and from other neurons to which it is connected. Each entry is associated with a weight representing the "strength" of the interneuron connection. Each calculation unit has its own transition or activation or transfer function which allows it to calculate its output state from the inputs and the weight of the associated connections [10].

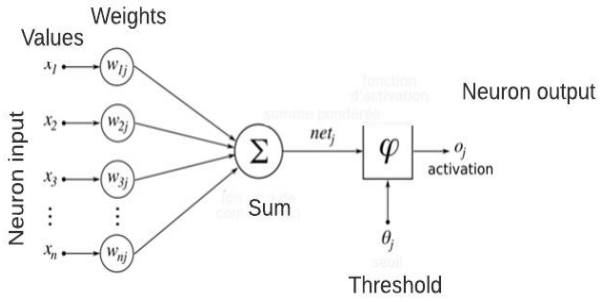

Fig. 7. Model of an artificial neuron.

The neuron behaviour is governed by the following equation:

$$S = X_1W_1 + X_2W_2 + \cdots + X_nW_n = \sum_{i=1}^{n} X_iW_i \quad (8)$$

S : the weighted sum;
$Y = f(x)$: the neuron output;
$X_1, X_2, \ldots, X_n$: the neuron inputs;
$W_1, W_2, \ldots, W_n$: the synoptic weights that control the passage rate of the input signal;
f : the transfer function;
Shows in Table 2, the commonly used transfer function for training neural networks. for multilayer networks with back-propagation algorithm. The most widely used transfer function is the log-sigmoid.

Table 2: The transfer function [12]

Name	**Input/output relation**
Hard limit	$f(x) = \begin{cases} 1 \; if \; x \geq 0 \\ 0 \; if \; x < 0 \end{cases}$
Symmetrical hard limit	$f(x) = \begin{cases} 1 \; if \; x \geq 0 \\ -1 \; if \; x < 0 \end{cases}$
linear	$Y = X$
Log-sigmoid	$Y = \frac{1}{1+e^{-X}}$
Hyperbolic tangent	$Y = \frac{e^{X}-e^{-X}}{e^{X}+e^{-X}}$

5.2 Learning of the neural network

Learning in a neural network is its developmental phase until the desired behavior is obtained. The weights of the connections are randomly initialized several times to calculate the output, until they reach their final value. The error is calculated and the weight correction will be applied if the goal is not reached. The learning algorithm is illustrated in Figure 8.

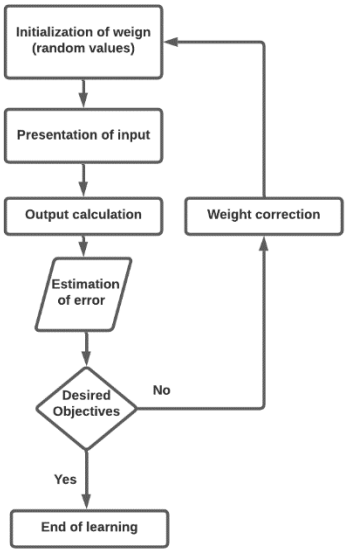

Fig. 8: The learning algorithm of a neural network

The data collected for the detection and characterization process are noisy, but the error tolerance capacity of the neural networks allows the detection system to differentiate the model from noise. This property is a huge advantage in fault detection and problem solving.

In this article, the Levenberg-Marquardt algorithm (LM) is proposed to perform the tasks of detection and classification of faults.

5.3 The setting and training

A network is driven on data through a learning mechanism that acts on the network components to achieve the desired task.

The network development process is in four phases:

- The collection of data made under Simulink using a file of each defect to change the input matrix.
- The generation of power, voltage and current errors contained in the input matrix through the MATLAB nstart block.
- The construction of the neural network, which is a two-layer network (201-24-142); three layers of size 3*201 inputs, 24 neurons in the hidden layer and 3*142 output.
- Finally, the artificial neuron network learning, uses the data contained in the input matrix.

- The setting of weight of input vectors and target vectors will be randomly divided into three sets as follows:
  - ✓ 70% will be used for training.
  - ✓ 15% will be used to validate the generalized network and stop the formation of the adjustment.
  - ✓ the remaining 15% will be used in an independent test of network generalization.

The network used is a two-layer feedforward network, with a sigmoid transfer function in the hidden layer and a linear transfer function in the production layer.

The simulation of the network in Figure 9 continue until the maximum error desired is reached after 1000 iterations, for a performance of 0.615 and a run time of 0.0004 seconds. The performance metric used by this Multi-layer Perceptron (MLP) is a cross-entropy (also called log loss) is a metric that should be minimized and not maximized in Figure 9. To this ANN code, we add the description code of the fault, by report with target in Table 1 above.

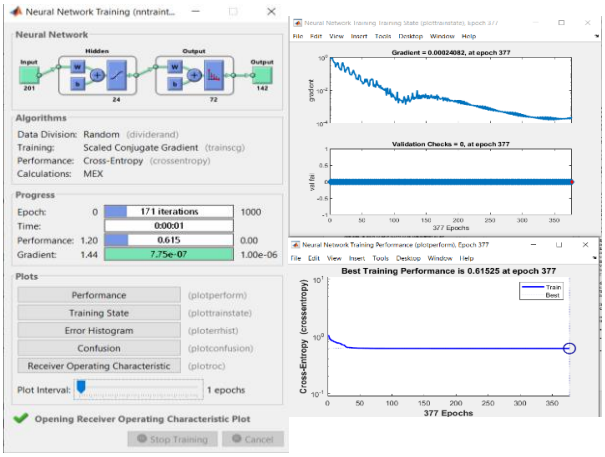

Fig. 9. ANN simulation result on Rs failure

Figure 10 shows the receiver operating characteristic curve, or ROC curve. In our case, it indicates a straight line corresponding to the first bisector, a random detection, indicating a high probability of detection for the two hypotheses, true or false. The area under the ROC curve (AUC, Area Under the Curve) gives an indicator of the quality of the prediction (1 for an ideal prediction, 0.5 for a random prediction).

Overall, we can consider an improvement for our diagnosis, either:

• Determine a threshold providing better performance, for a COR above the first bisector;

• determine better measurement conditions, for better overall performance of the COR curve.

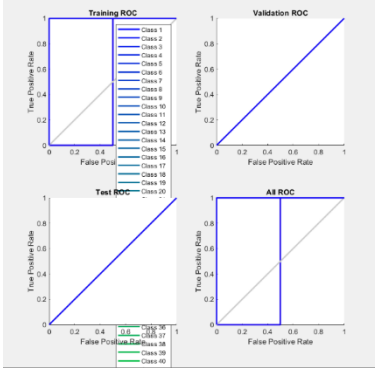

Fig. 10. ANN simulation results minimum gradient

6 Simulation and interpretation

We have chosen by experience and experimentally a fault detection threshold of (0.001), because it offers relatively satisfactory results and avoids false detections. Then, we pass the output matrix under an nnstart algorithm for fault detection and classification.

6.1 Healthy mode or no defaults

From an input matrix derived from a healthy mode of operation, we gave a threshold of 0.1 and obtained the following identification and localization in Figure 11:

```
>> spvrnaModeSain1

performance =

    0.6152

000 : Healthy mode
111 : Fault nature is Unknown
```

Fig. 11. Diagnosis in a healthy mode

6.2 Default on Rs

From an input matrix derived from a gradient mode of operation on Rs, we gave a threshold of 0.0001 and obtained the identification and location below in Figure 12. In the figure 5, we have a few deviation.

```
>> spvrnamodesain6

performance =

    0.6152

000 : Healthy mode
011 : Mismatch type partial shade, or dirt
100 : Bypass or Mismatch type Rp or Rs
```

Fig. 12. Diagnosis due to variation in Rs

6.3 Rsh defect

From an input matrix derived from a gradient mode of operation on Rsh, we gave a threshold of 0.0001, because in Figure 5, we have a few vertical deviation and obtained the identification and location below in Figure 13:

```
>> spvrnamodesain6

performance =

    0.6152

000 : Healthy mode
010 : Short-circuited or reverse module
100 : Bypass or Mismatch type Rp or Rs
```

Fig. 13. Diagnosis due to variation in Rsh

6.4 Temperature fault

From an input matrix derived from a gradient mode of operation on T, we gave a threshold of 0.0001 we have current or voltage which decrease and obtained the identification and location below in Figure 14:

```
>> spvrnamodesain6

performance =

    0.6152

000 : Healthy mode
011 : Mismatch type partial shade, or dirt
100 : Bypass or Mismatch type Rp or Rs
```

Fig. 14. Diagnosis due to variation in T

6.5 Summary

The diagnosis technique by ANN uses a database to detect and classify the faults defined in the signature matrix of Table 1, according to the previously defined threshold. The learning of the ANN is quite simple and allows to classify the faults, to improve the results obtained and

the percentage of detection if necessary. To improve its performances, we can do one of the following:

- Train again;
- Increase the number of neurons;
- Choose a larger training data set, which takes a lot more time and patience to build such a database.

On the one hand, if the overall learning performance is good, but the testing performance is significantly poor, then the number of neurons should be reduced. To have poor performance, increases the number of neurons.

On the other hand, the choose of the threshold is difficult because the modification of the values of a parameter linked to a known fault, can appear under the nature of another fault. This leads to false alarms and poor detection of a certainly major fault.

7 Conclusion

From the results obtained, we can say that the ANN approach is based on a database to detect, classify and isolate faults. It is a relatively simple technique that does not require complex programming languages.

The analysis of the simulation results shows that the ANN are sufficiently efficient for the diagnosis and that they remain a simple and suitable technique to ensure a good diagnosis for a conditional or preventive maintenance in a PVG. Locating the R_s, R_{sh}, T, G or I_{ph} type of fault will no doubt make it possible to take the appropriate measures to restore the PVG to the best operating conditions.

Depending on the failure area in Fig. 5, the error value is small or large. That is why we have to adjust the threshold every time in our classification algorithm, shown in Figures 10 to 13. This part of the diagnosis also opens up huge improvements for the prognosis over the remaining life or RUL of our PVG, but requires a database large enough for the application of neural network analysis.

The use of this artificial intelligence method in the field of automation for the diagnosis of a complex industrial system is very commendable. The prospects are quite good, but only the use of an automatic database of residuals, built over a long period with patience, will allow a diagnosis in real time and without false interpretation of the anomalies of the PVG, and in relation to the parameters. incriminated. This will allow of course technicians to better maintain PVG, but especially engineers to design on-board and autonomous equipment able of making decisions in the direction of increasing remaining useful life (RUL). This research work is necessary both for the search for clean energy accessible to all with an optimal return on investment as stipulated in article 7 of the United Nations charter for sustainable development.

References

[1] G. Li, Yi Jin, M.W. Akram, Xiao Chen, J. J. Application of bio-inspired algorithms in maximum power point tracking for PV systems under partial shading conditions – A review. Renewable and Sustainable Energy Reviews 81 (2018) 840–873

[2] J. Jurasz, A. Kies, P. Zajac. Synergetic operation of photovoltaic and hydro power stations on a day-ahead energy market. Energy 212 (2020) 118686

[3] A. Mellit, G.M. Tina, S.A. Kalogirou. Fault detection and diagnosis methods for photovoltaic systems: A review. Renewable and Sustainable Energy Review 91 (2018) 1–17

[4] L. Bun. Détection et localisation de défauts pour un système PV. Thèse de doctorat, Université de Grenoble, France (2011).

[5] Telidjane, M. Modélisation des panneaux photovoltaïques et adaptation de la cyclo-stationnarité pour le diagnostic. Thèse de doctorat, Université de Jean Monnet Saint-Etienne, Lyon, France (2017).

[6] A. Ndiaye. Étude de la dégradation et de la fiabilité des modules photovoltaïques – Impact de la poussière sur les caractéristiques électriques de performance. Sciences de l'ingénieur [physics]. Ecole Supérieure Polytechnique (ESP) - UCAD, (2013).

[7] J. Bishop. Computer Simulation of the Effects of Electrical Mismatches in Photovoltaic Cell Interconnection Circuits. Solar Cells, 25 :73_89 (1988).

[8] D. Picault, B. Raison, S. Bacha, J. Aguilera, et J. De La Casa. Changing Photovoltaic array interconnections to reduce mismatch losses: a case study. 2010 9th International Conference on Environment and Electrical Engineering :37_40 (2010).

[9] R. Doumane. Modélisation du Vieillissement d'un Module Photovoltaïque. Thèse de Doctorat, Université M'hamed Bougara Boumerdes Algérie (2011).

[10] D. Kumar, P. Mishra, A. Ranjan, D. K. Dheer, L. Kumar. A simplified simulation model of silicon photovoltaic modules for performance evaluation at different operating conditions. Optik - International Journal for Light and Electron Optics 204 (2020) 164228

[11] A.E. T. Maamar, S. Ladjouzi, R. Taleb and Y. Kacemi. Détection et classification de défauts pour un GPV : Etude comparative entre la méthode de seuillage et réseaux de neurones. *Revue des Energies Renouvelables Vol.21 N°1 45-53(2018).*

[12] A.E. T. Maamar, S. Ladjouzi, R. Taleb and Y. Kacemi. Detection and classification of faults in a photovoltaic system using the neuronal approch ISSN 2676-248X (2019)

[13] L. Bun, B. Raison, G. Rostaingy, S. Bacha, A. Rumeau_, A. Labonne. Development of a Real Time Photovoltaic Simulator in Normal and Abnormal Operations. G2ELAB - Grenoble Electrical Engineering Laboratory, Grenoble University, France.

[14] A. Mellita, G.M. Tinac, S.A. Kalogiroud. Fault detection and diagnosis methods for photovoltaic systems: A review. Renewable and Sustainable Energy Reviews 91 (2018)